Supporting Information

Exploiting a Global Regulator for Small Molecule Discovery in *Photorhabdus luminescens*

Renee Kontnik,* Jason Crawford,* and Jon Clardy†

Department of Biological Chemistry & Molecular Pharmacology, Harvard Medical School, 240 Longwood Avenue, Boston, MA 02115.

***** These authors contributed equally to this work.
† To whom correspondence may be addressed.

Corresponding author: Jon Clardy, 240 Longwood Avenue, C-643, Boston, MA 02115.
Ph: 617-432-2845. Fax: 617-432-6424. Email: jon_clardy@hms.harvard.edu

Contents:

Supplemental Methods

Preparation of *lrp* deletion construct. The entire coding sequence from start to stop codons of *lrp* (locus tag: Plu1600; Protein Accession: NP_928891) was excised by allelic-exchange mutagenesis to generate a markerless deletion mutant. The exchange sequence for *lrp* consisted of ~1 kB of upstream and downstream genome sequence fused by overlap extension PCR. The first fragment was amplified with primer pairs Lrp-A5 and Lrp-A3 (Table S1), and the second fragment was amplified with primer pairs Lrp-B5 and Lrp-B3. The two products were used as templates in the final PCR, using primer pairs Lrp-A5 and Lrp-B3, thereby fusing the two pieces. The full-length *lrp* exchange sequence was digested with SacI, inserted into the corresponding site in pDS132, and verified by restriction analysis (pDΔLrp). Cloning was carried out in *E. coli* strain WM3618 lambda *pir*.

Preparation of *hexA* knockout construct. Because markerless deletion attempts of *hexA* failed in our hands, an internal *hexA* (locus tag: Plu3090; Protein Accession NP_930322) gene fragment was amplified using HexA-iKO5 and HexA-iKO3, digested with SacI, and inserted into the corresponding site in pDS132 (pDiHexA) for plasmid integration. Cloning was carried out in *E. coli* strain WM3618 lambda *pir*. Ligation products in both directions were successfully taken forward to insertionally inactivate *hexA* by pDiHexA plasmid integration containing a chloramphenicol resistance marker.

Genetic inactivation of *lrp* and *hexA* in *P. luminescens*. The pDS132 deletion constructs (pDΔLrp or pDiHexA) were transformed into the diaminopimelic acid (dap) auxotroph donor strain, *E. coli* WM6026 lambda pir (*28*), by heat-shock transformation (*29*). The donor *E. coli* and recipient WT *P. luminescens* TT01 were grown to OD_{600} = 0.6–0.8, mixed in a 2:8 (donor:recipient) ratio, filtered through a 0.2 μM sterile filter, and allowed to filter mate on LB agar supplemented with 0.3 mM dap overnight at 30 °C. The mating mixture was resuspended in liquid LB and plated on LB chloramphenicol (25 μg mL^{-1}) plates supplemented with 0.3% pyruvate, but lacking supplemental dap. Markerless *lrp* mutants were then selected on LB sucrose (5%) plates for SacB counter-selection. Positive deletions were identified by colony PCR and sequence verified. For insertional inactivation of *hexA*, agar plates used for filter mating and all subsequent plating steps were also supplemented with 100 mM L-proline. Successful *hexA* plasmid integrants were identified by colony PCR and sequence verified. No SacB counter selection was performed.

Identification of successful markerless *lrp* deletion mutants. *P. luminescens* colonies on SacB counterselection LB-sucrose medium were analyzed by colony PCR using Lrp5-genome and Lrp3-genome. Successful mutants exhibited an ~2 kB PCR product indicative of sequence exchange and the removal of the *lrp* sequence. The colonies were restreaked three times on the counterselection medium to remove any potential traces of WT and again analyzed by PCR. The ~2 kB PCR product was cloned into pCR2.1 TOPO (Invitrogen) and sequence verified.

Identification of successful *hexA* insertional knockouts. *P. luminescens* colonies growing on the chloramphenicol selection plates were analyzed by PCR. Primers were selected on the plasmid backbone and in the genome to verify insertion at both ends. Figure S4 illustrates the primer pairs HexA5-genome/pDS-vector1 and HexA3-genome/pDS-vector2 to identify successful pDiHexA plasmid integrants. The two PCR products were cloned into pCR2.1 TOPO (Invitrogen) and

sequence verified. The mutants were restreaked three times on LB chloramphenicol (25 μg mL^{-1}) plates supplemented with 0.3% pyruvate and 100 mM L-proline to remove potential traces of WT, although without selection reversion to WT could occur (Figure S4). For the reverse direction knockout construct (not illustrated), primer pairs included HexA5-genome/pDS-vector2 and HexA3-genome/pDS-vector1.

Metabolite analysis by HPLC. Organic extracts obtained from WT and Δ*hexA* strains of *P. temperata* and *P. luminescens* were separated over a Discovery RP-amide C16 (25 cm x 4.6 mm, 5 μM, Supelco) HPLC column with an acetonitrile:water gradient at 1 mL min^{-1}: 0–2 min, 10 % acetonitrile; 2–10 min, 10–50% acetonitrile; 10–25 min, 50–75% acetonitrile.

Table S1. Oligonucleotide sequences used in obtaining *lrp* and *hexA* knockouts in *P. luminescens.*

Primer	Sequence
Lrp-A5	gtaagagctc-cagatataaggcctcttctaccgcgg
Lrp-A3	ctgtacatttttggtaagatt-cttgttgatctctctttattttcctacacccat
Lrp-B5	taaagagagatcaacaag-aatcttaccaaaaatgtacaggtgcaaaac
Lrp-B3	gtaagagctc-gaatttcaggttcagcatcaatattagcc
Lrp5-genome	tcacggcgatgaattaggtgaacttc
Lrp3-genome	gctgagactggacaataccatcatctgatg
HexA-iKO5	agtaaatc-gagctc-ttcttacagagcatggtcttcaacttcttgg
HexA-iKO3	agtaaatc-gagctc-tttgcatttccaaaggacgggcag
HexA-5genome	agagtcttaccttatcttggtaaaaaaagtcg
HexA-3genome	aatgcccagtgatgggcaaagag
pDS-vector1	tatctcatttcactaaataatagtgaacggcagg
pDS-vector2	tttgagtgacacaggaacacttaacggc

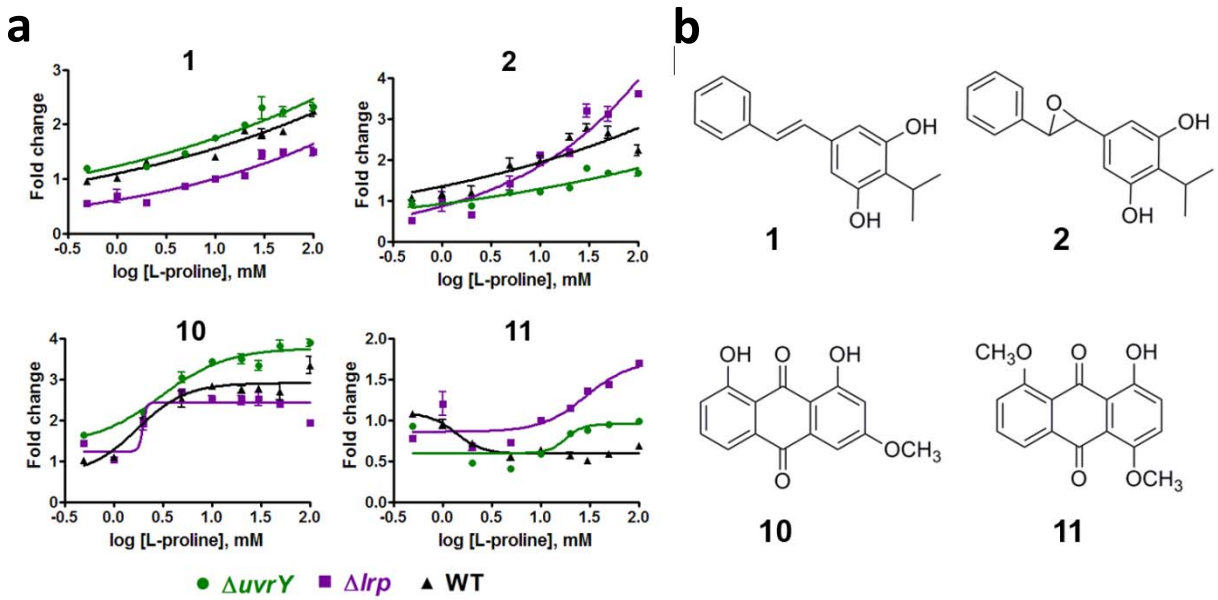

Figure S1. Metabolomic profiling of *P. luminescens* Δ*uvrY* and Δ*lrp*. (a) Fold change in metabolite production of the two mutants compared to wild type (WT) with increasing concentration of proline. Numbers above curves refer to structures in (b). No substantial change in production of any of the four major *P. luminescens* secondary metabolites from organic extracts was observed in these mutants.

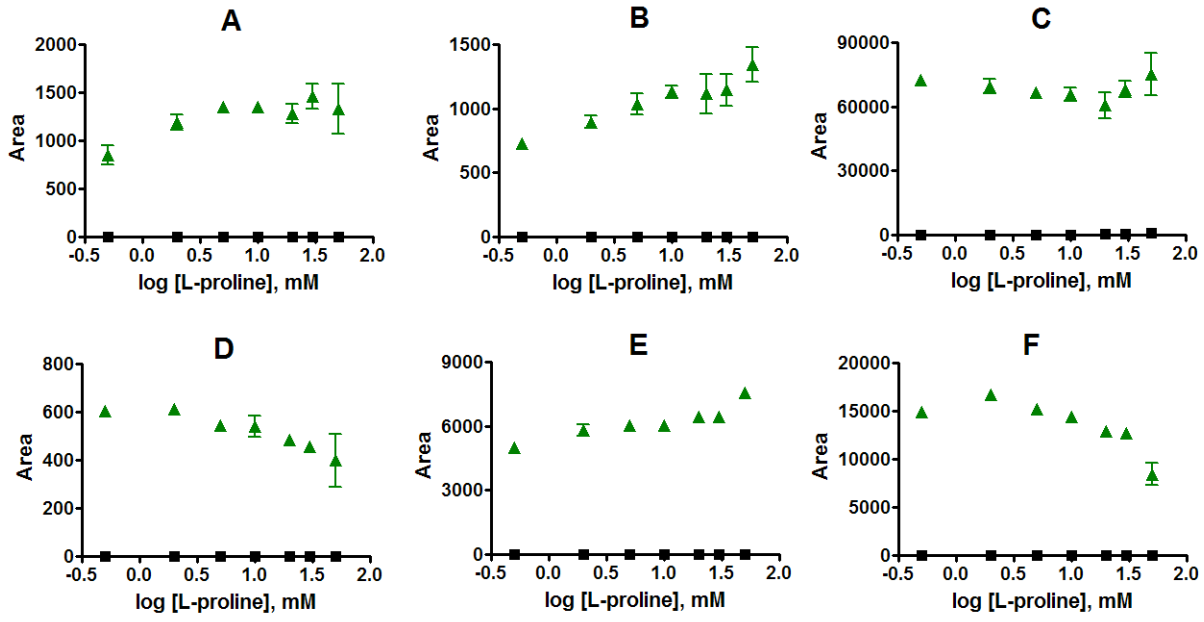

Figure S2. Metabolomic profiling of *P. temperata* Δ*hexA* (green ▲) vs. WT (black ■). Plots refer to individual metabolites (area of peaks on HPLC traces versus increasing concentration of proline). Metabolites **A**, **B**, and **C** are stilbene derivates **1**, **2**, and **3**, respectively (Figure 2). Metabolites **D** – **F** were not fully characterized but are known to be isomers of the known anthraquinones **10** and **11** based on their signature UV-visible chromophores and mass.

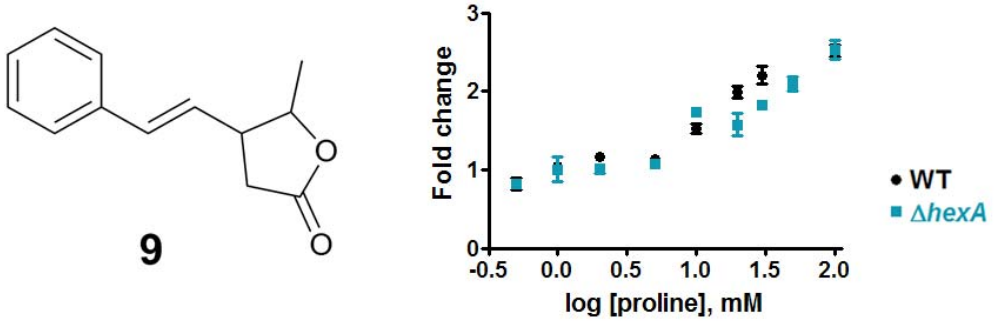

Figure S3. Production of **9** in *P. luminescens* Δ*hexA* vs. WT. Metabolomic profiling of **9** showed that production of this compound is unchanged in *P. luminescens* Δ*hexA* compared to WT. This metabolite is structurally the most divergent from the stilbenes and may therefore require other biosynthetic genes and serve other biological functions.

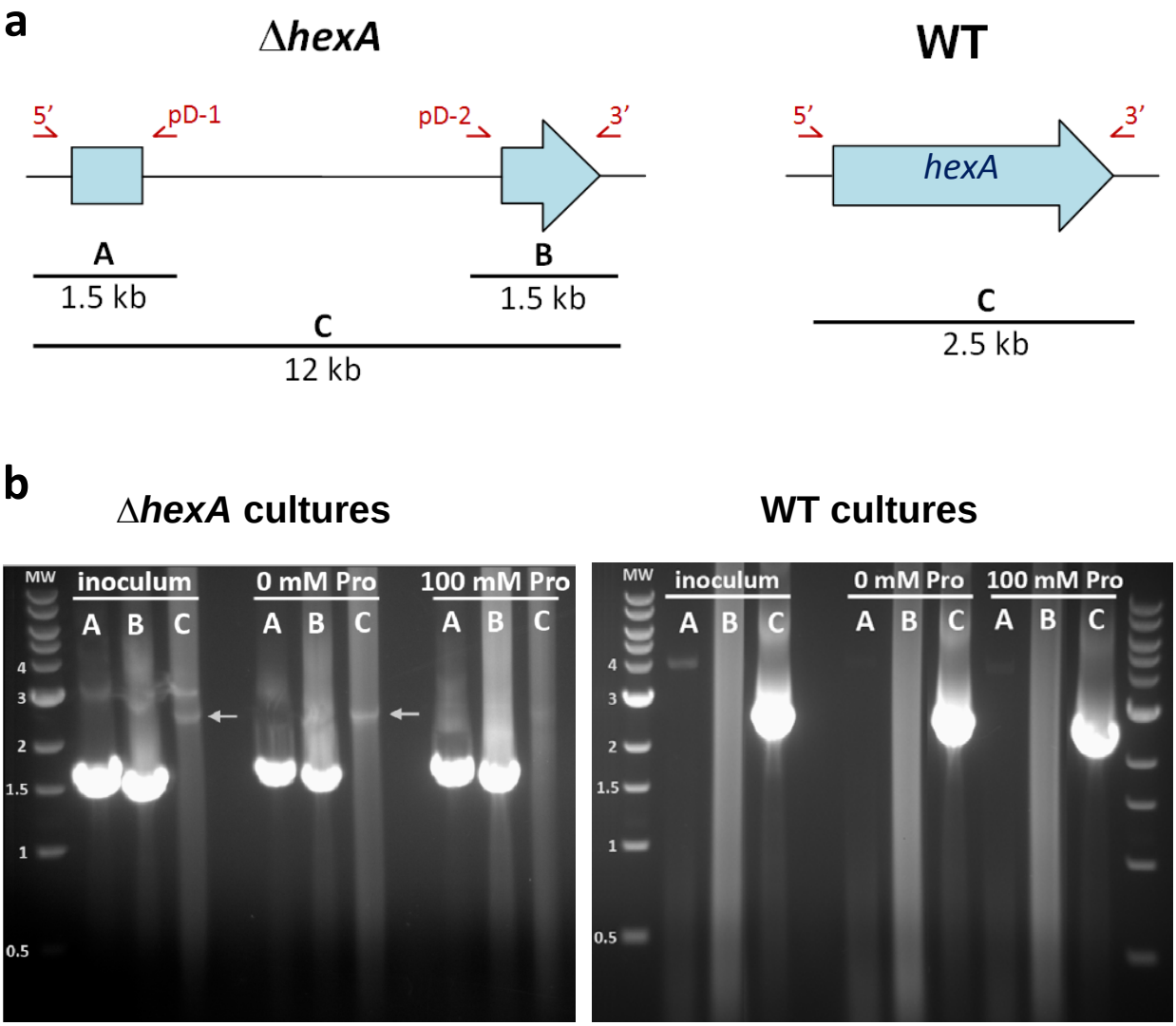

Figure S4. Assessing reversion of *P. luminescens* Δ*hexA* by PCR. Due to the difficulty in propagating the *hexA* inactivant, we evaluated whether reversion was detectable in our metabolite analysis. (a) Three primer sets were designed to assess reversion of *P. luminescens hexA* insertional inactivants back to WT. Fragments A and B (both 1.5 kb) should be present only in the Δ*hexA* insertional mutant and not in WT, as one primer is derived from the inserted sequence in both cases. PCR with the 5' and 3' primers should give rise to a 2.5 kb band in WT. With these primers, the ~12 kB product was not observed in Δ*hexA* due to the length of the insert and the prohibitive PCR method used (short extension time). (b) Agarose gel illustrating results of the PCR. Δ*hexA* cultures exhibit low levels of the 2.5 kb fragment indicative of WT *hexA* (arrows), and supplementation of L-proline appears to stabilize the *hexA* inactivation.

Table S2. ^{1}H and ^{13}C data for **4 – 9** in CD_3OD. Chemical shifts (δ) in ppm.

atom	4		5		6	
	δ_C	δ_H (mult, *J* [Hz])	δ_C	δ_H (mult, *J* [Hz])	δ_C	δ_H (mult, *J* [Hz])
1	137.1		141.4		137.2	
2	106.1	6.34 (s)	106.7	6.26 (s)	106.7	6.30 (s)
3	157.2		156.1		156.2	
4	121.5		120.1		120.7	
5	157.2		156.1		156.2	
6	106.1	6.34 (s)	106.7	6.26 (s)	106.7	6.30 (s)
7	126.7	6.21 (d, 16.1)	85.3	4.67 (d, 6.3)	76.1	5.82 (s)
8	130.2	6.67 (d, 16.1)	85.5	4.53 (d, 6.4)	199.1	
9	133.8		140.1		134.8	
10	127.2	5.83[a]	128	7.29[a]	128.5	7.95 (d, 7.9)
11	25.9	2.82[a]	128	7.27[a]	128.4	7.41 (t, 8.0)
12	123.7	5.73 (d, 10.2)	128	7.27[a]	133.0	7.53 (t, 7.3)
13	123.7	5.82[a]	128	7.27[a]	128.4	7.41 (t, 8.0)
14	25.9	2.85[a]	128	7.29[a]	128.5	7.95 (d, 7.9)
15	23.2	3.46 (m, 7.0)	25.0	34.6 (m, 7.2)	24.3	3.40 (m, 7.0)
16	20.8	1.26 (d, 7.0)	20.5	1.27 (d, 7.2)	19.7	1.24 (d, 7.0)

atom	7		8		9	
	δ_C	δ_H (mult, *J* [Hz])	δ_C	δ_H (mult, *J* [Hz])	δ_C	δ_H (mult, *J* [Hz])
1	140.7		140.8		49.2	2.95 (m)
2	108.4	6.87 (s)	106.7	6.00 (s)	82.7	4.42 (dq, 9.2, 6.4)
3	157.6		156.2		178.1	
4	128.5		120.7		36.8	2.69 (dd, 17.3,
5	157.6		156.2		134.3	6.20 (dd, 15.7, 8.3)
6	108.4	6.87 (s)	106.7	6.00 (s)	128.0	6.58 (d, 15.7)
7	199.8		88.8	3.95 (d, 7.9)	138.1	
8	77.0	5.90 (s)	78.1	4.62 (d, 7.9)	127.2	7.41 (d, 8.3)
9	140.7		136.5		127.9	7.30 (t, 7.4)
10	128.5	7.39 (d, 8.4)	127.5	7.10 (d, 7.3)	129.4	7.22 (t, 7.2)
11	128.5	7.33 (t, 7.2)	127.5	7.15-7.15[a]	127.9	7.30 (t, 7.4)
12	129.7	7.27 (t, 7.2)	127.5	7.15-7.15[a]	127.2	7.41 (d, 8.3)
13	128.5	7.33 (t, 7.2)	127.5	7.15-7.15[a]	18.9	1.40 (d, 6.3)
14	128.5	7.39 (d, 8.4)	127.5	7.10 (d, 7.3)		
15	26.1	3.49 (m, 7.0)	24.3	3.40 (m, 7.0)		
16	19.8	1.26 (d,	19.7	1.24 (d, 7.0)		

[a] Overlapped peaks

Figure S5

4, ^{1}H-NMR (600MHz, CD_3OD)

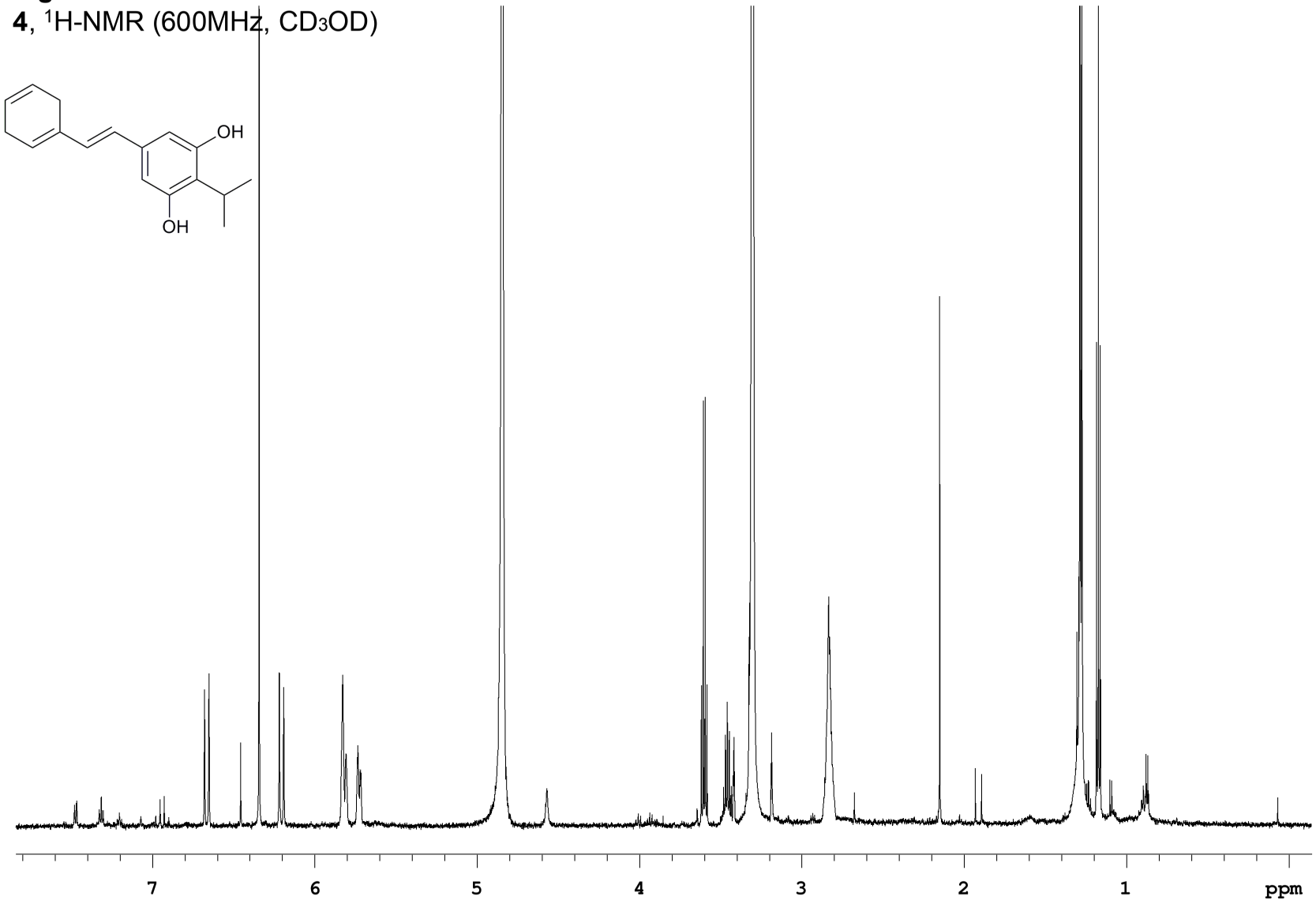

Figure S6

4, gCOSY (600MHz, CD_3OD)

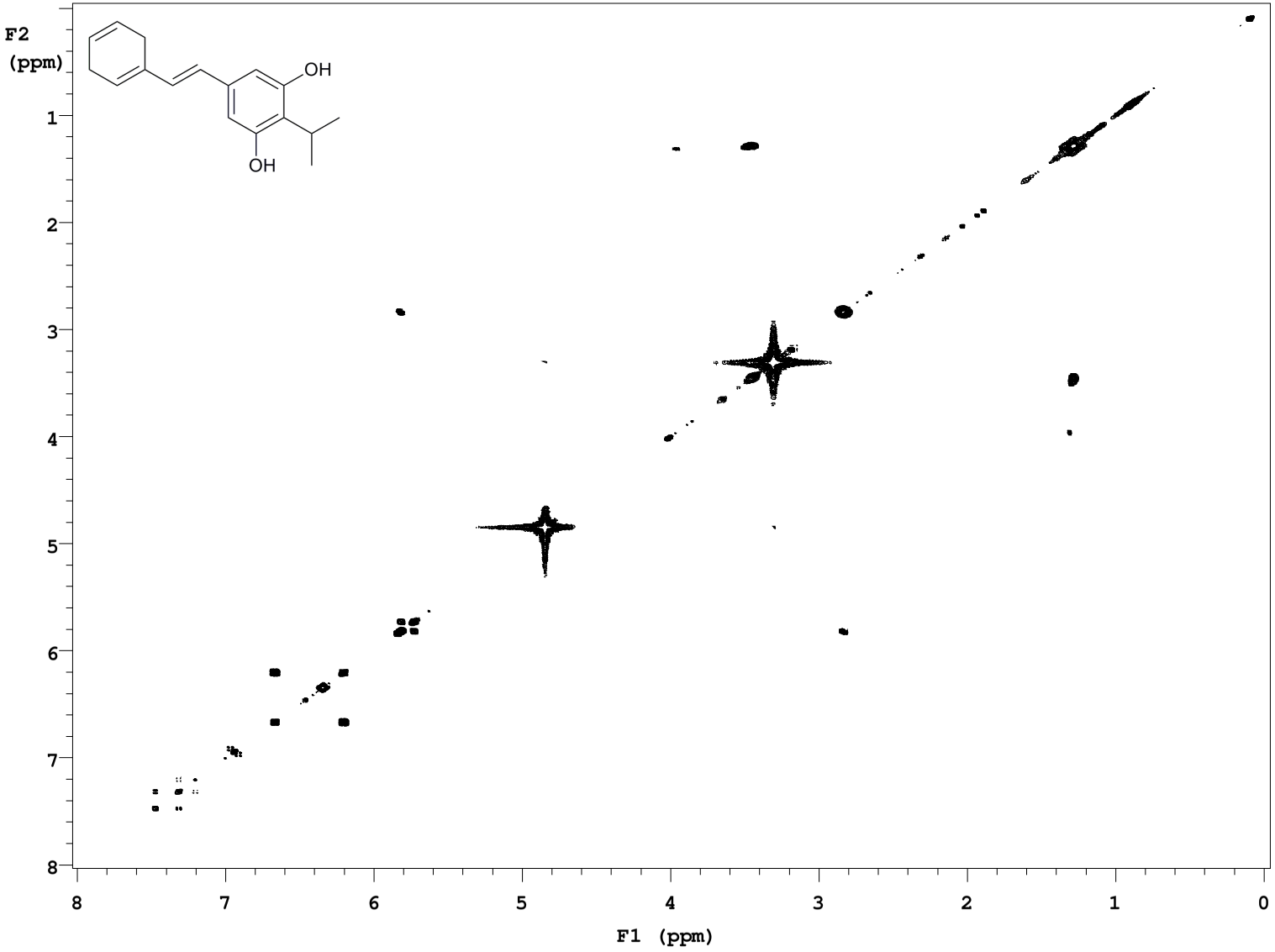

Figure S7

4, gHSQC (600MHz, CD_3OD)

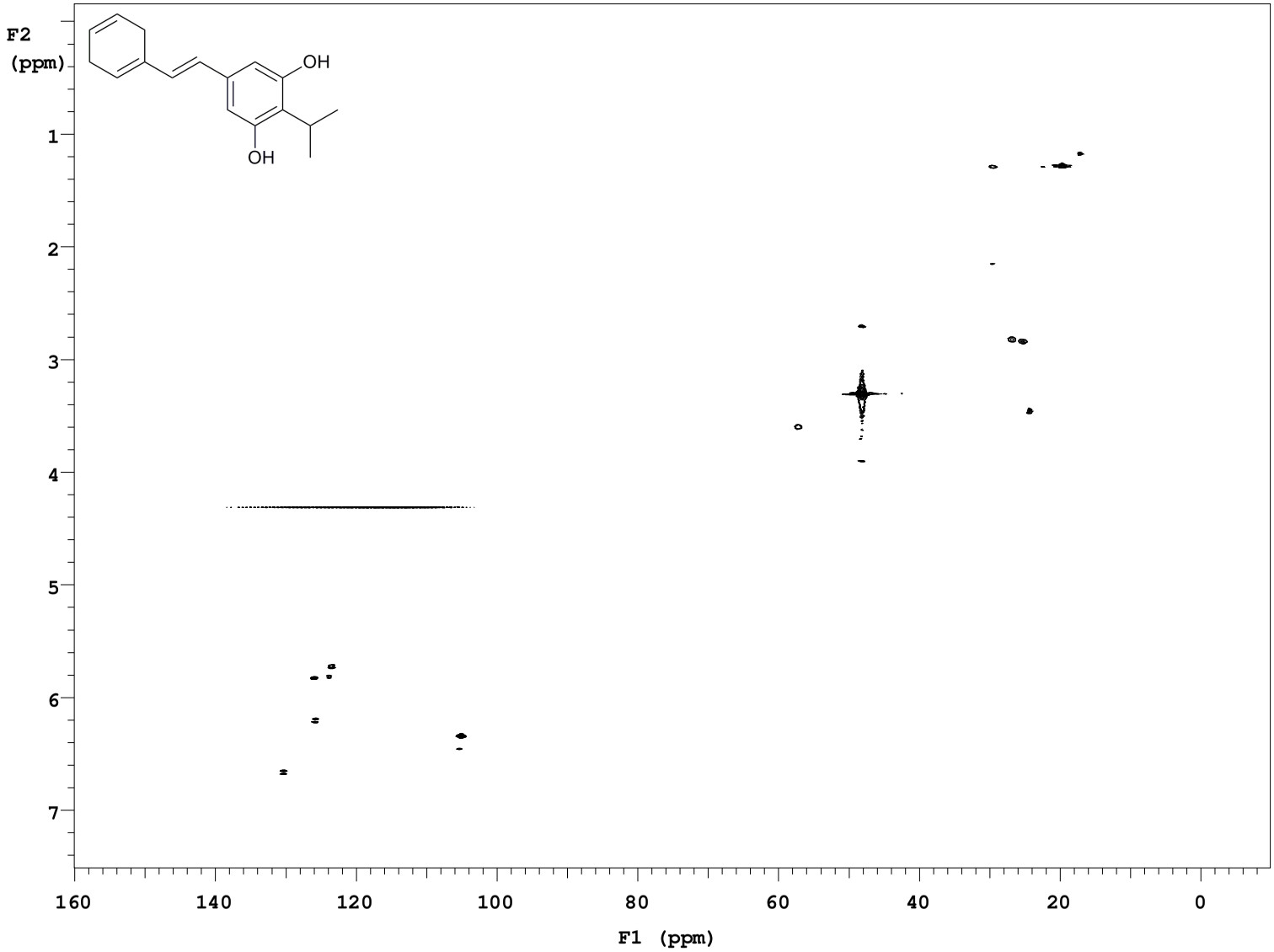

Figure S8

4, gHMBC (600MHz, CD_3OD)

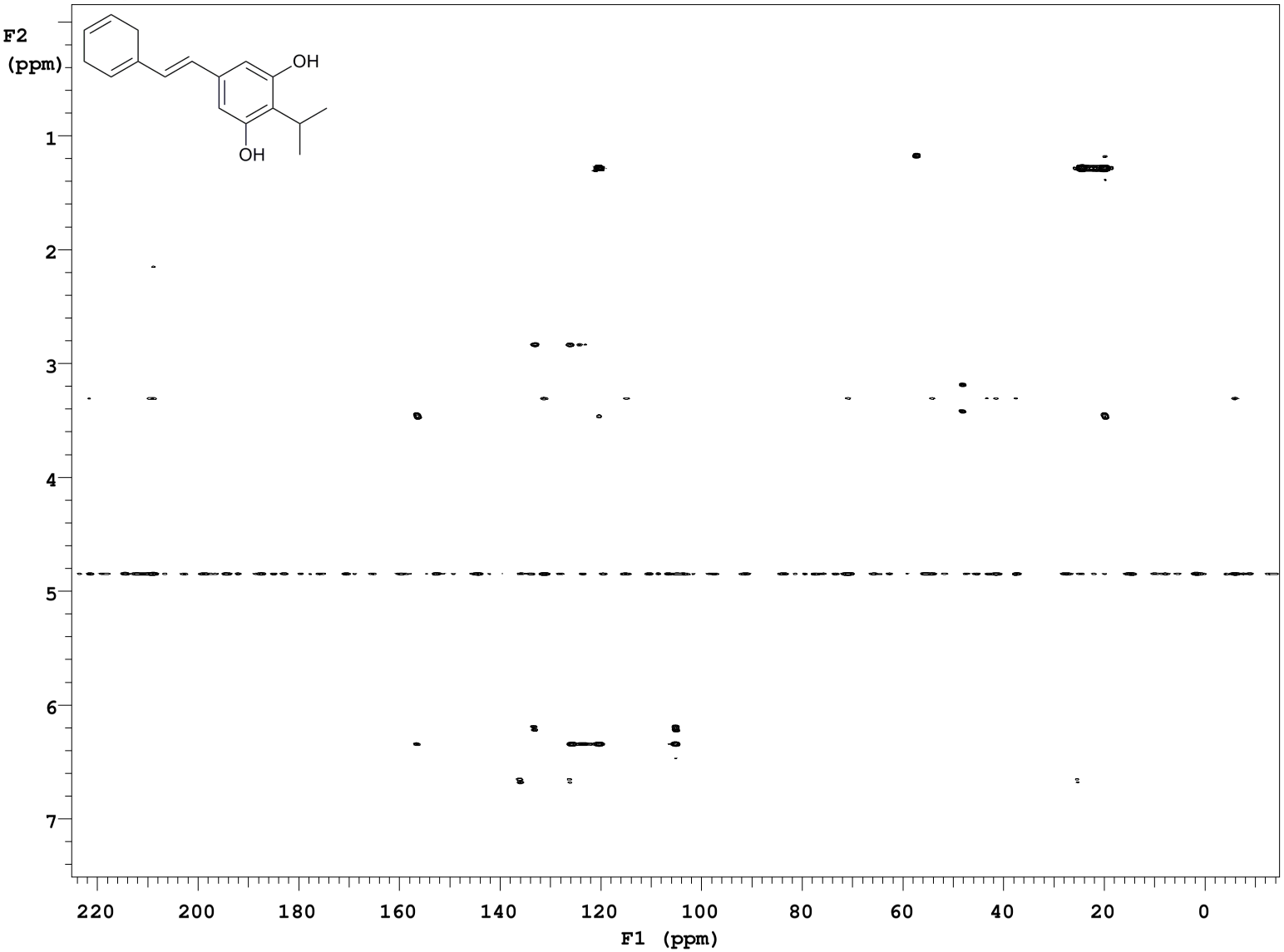

Figure S9

4, ROESY (600MHz, CD_3OD)

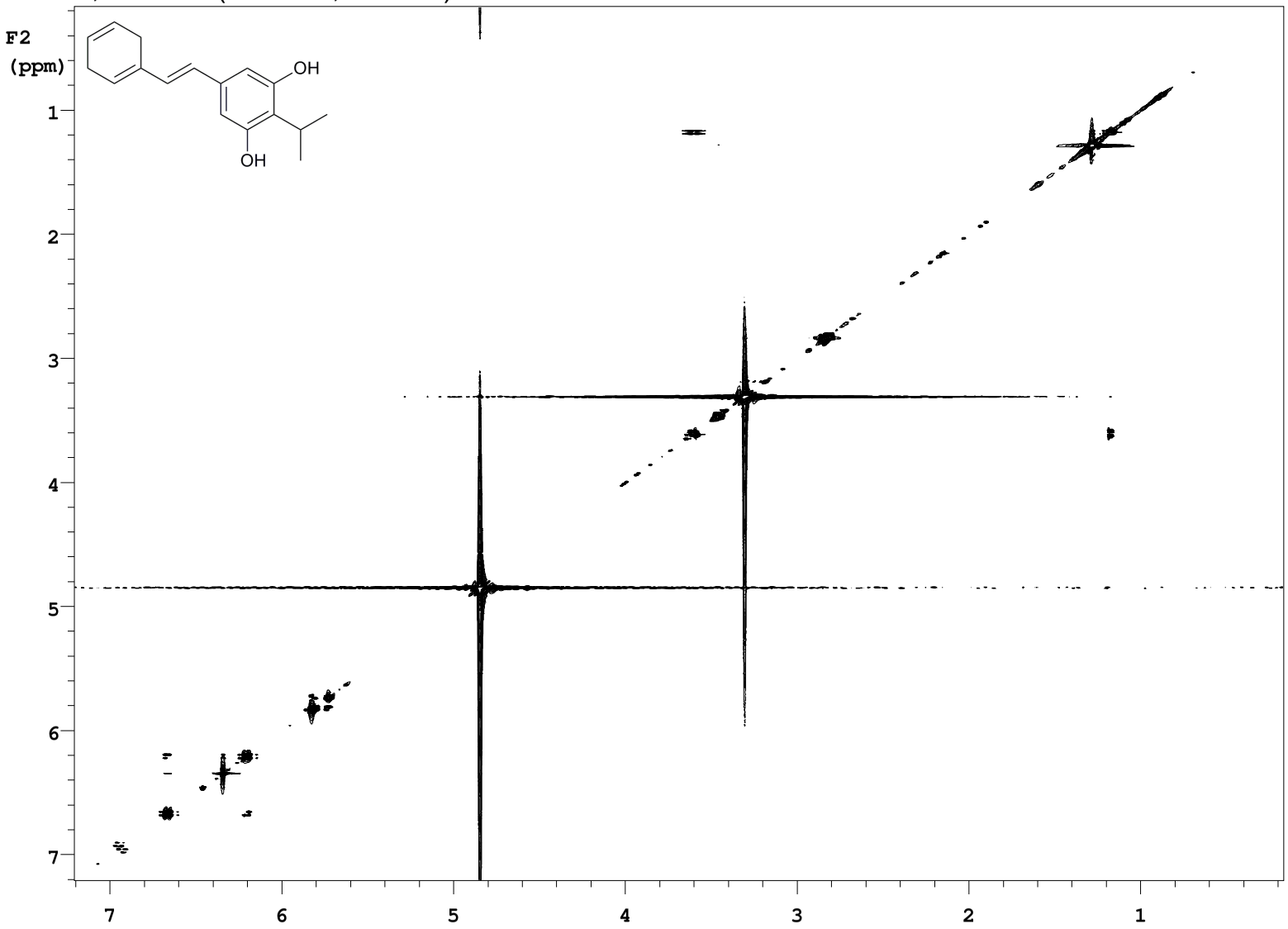

Figure S10

5, ^{1}H-NMR (600MHz, CD_3OD)

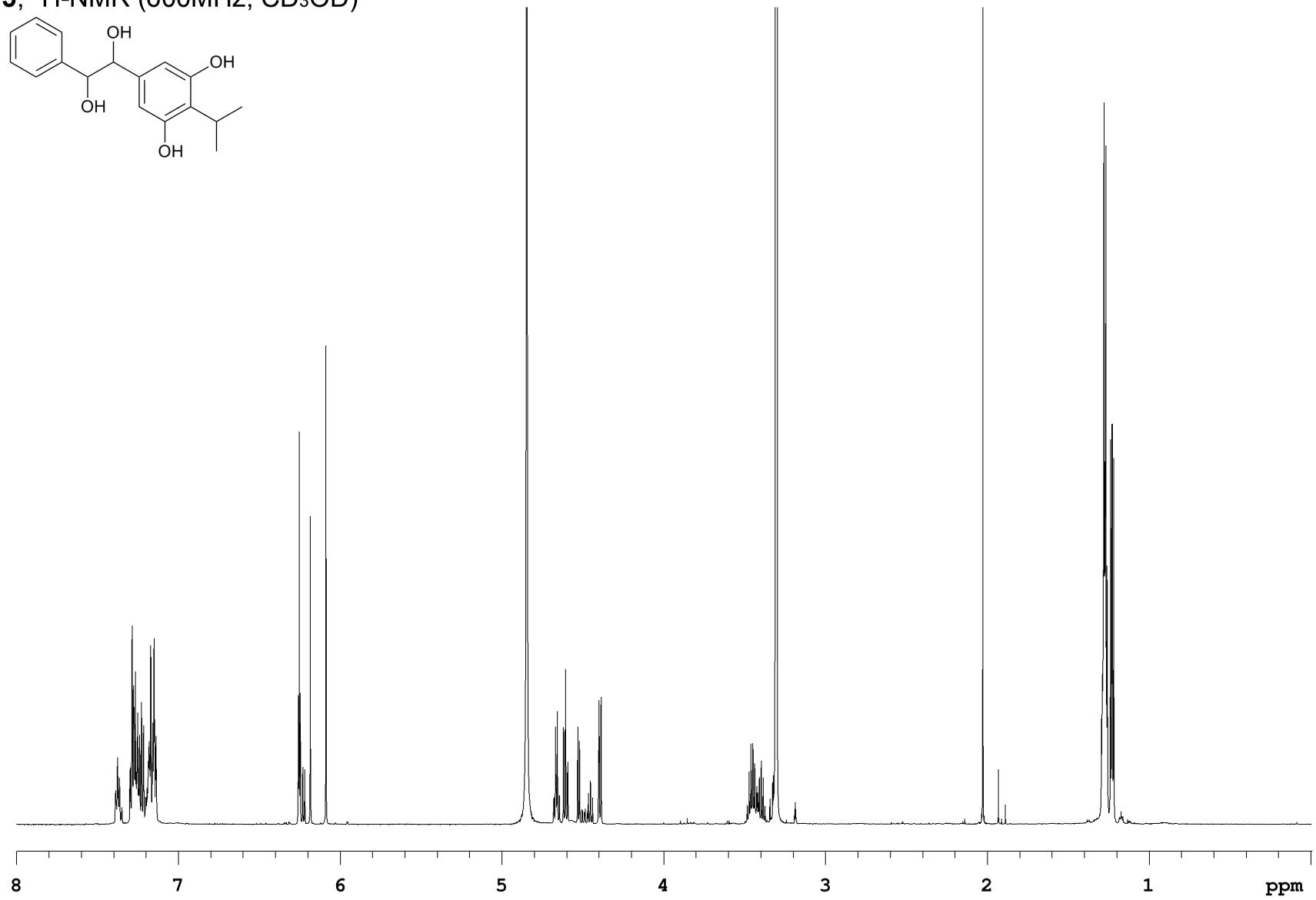

Figure S11
5, gCOSY (600MHz, CD_3OD)

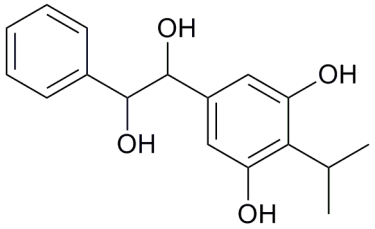

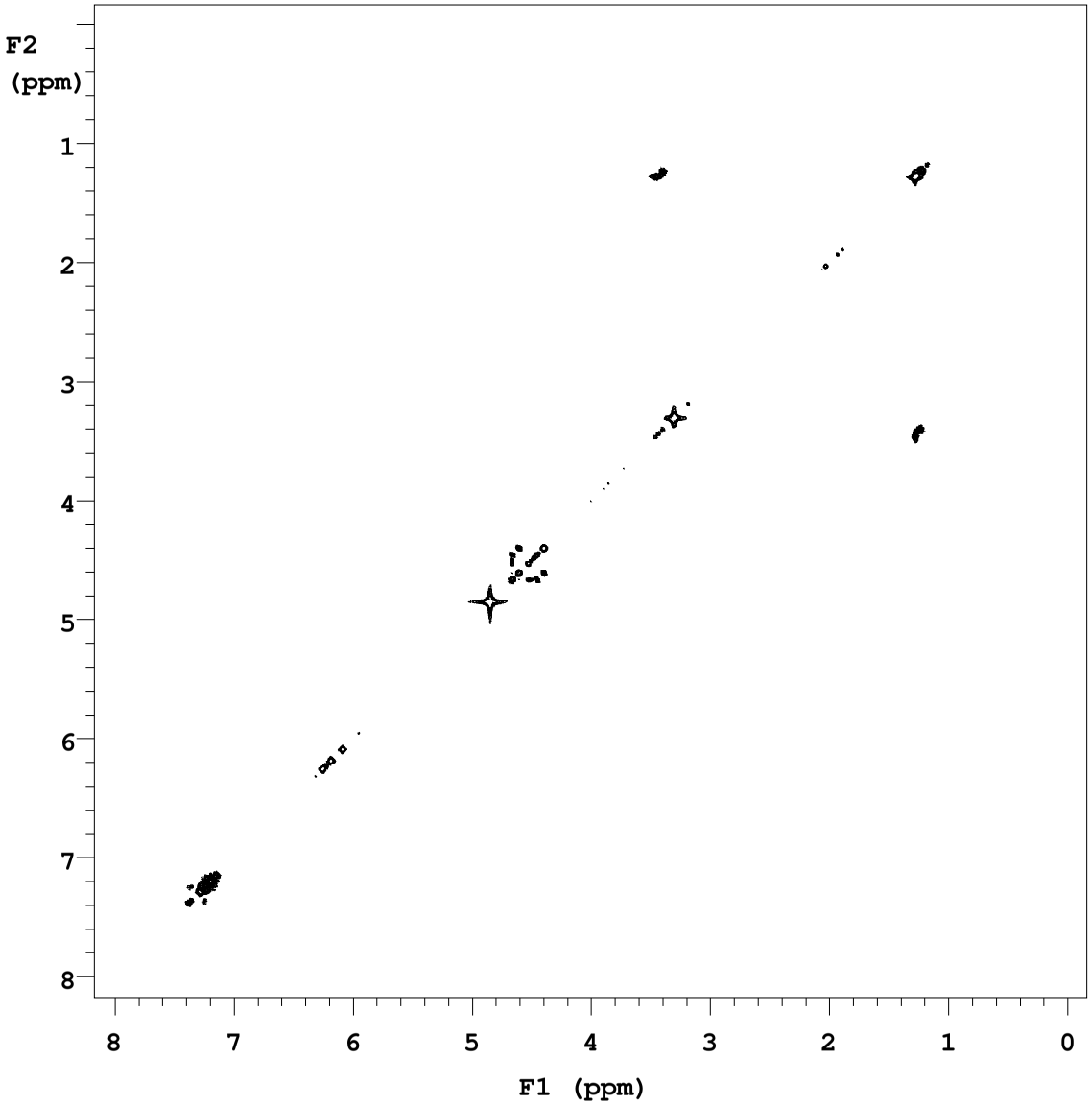

Figure S12

5, gHSQC (600MHz, CD_3OD)

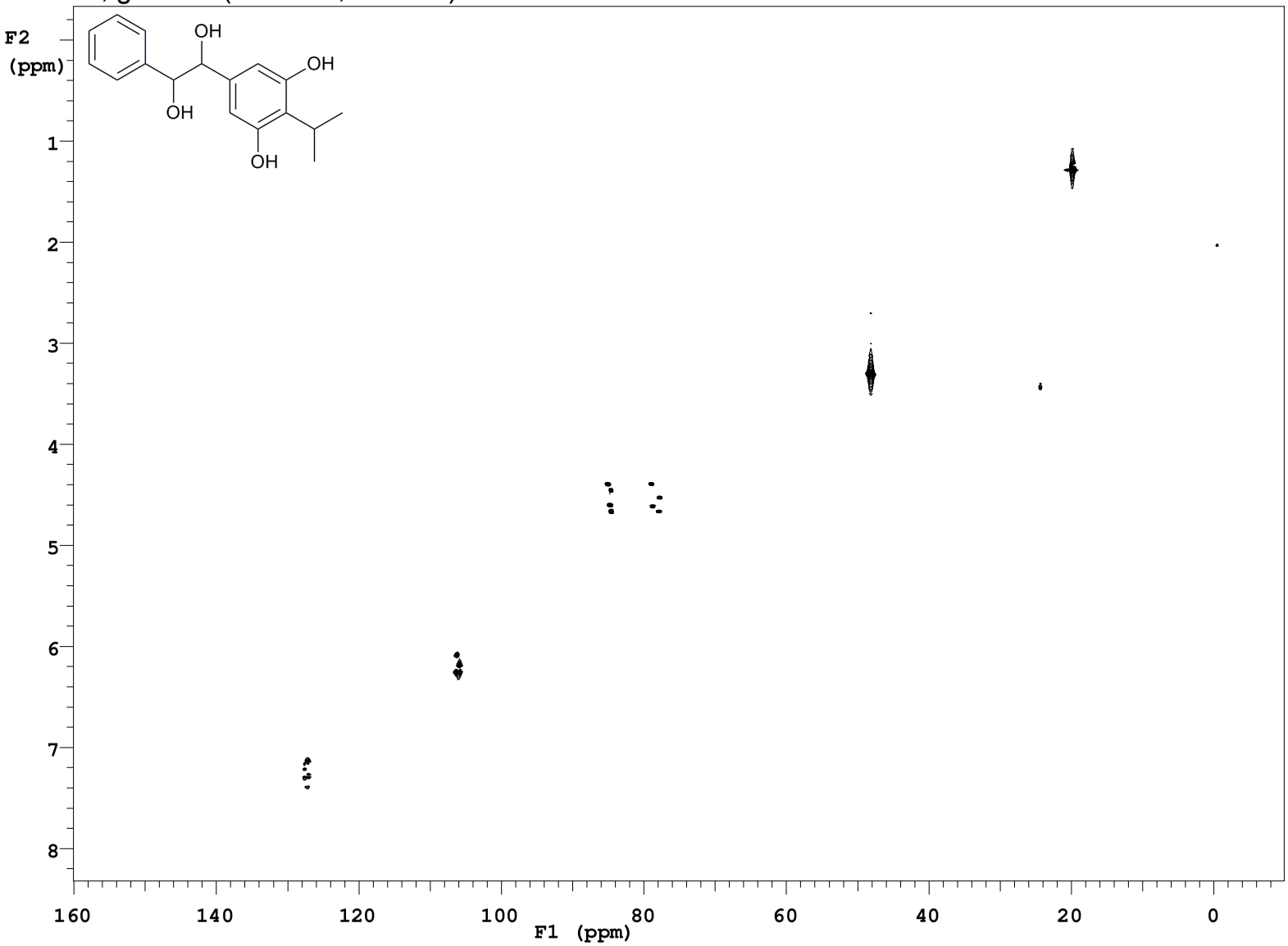

Figure S13

5, gHMBC (600MHz, CD_3OD)

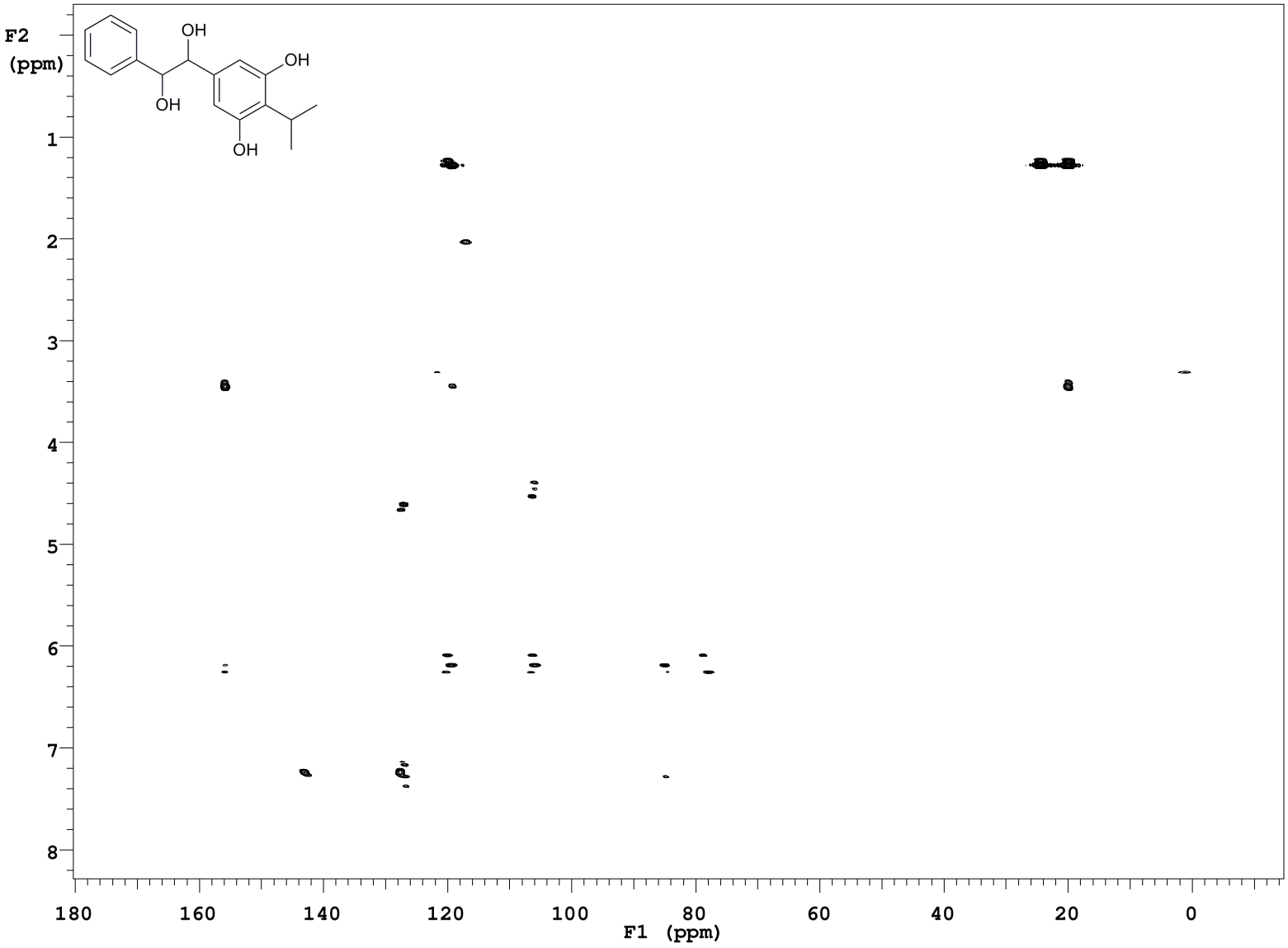

Figure S14

6 & **8**, ^{1}H-NMR (600MHz, CD_3OD)

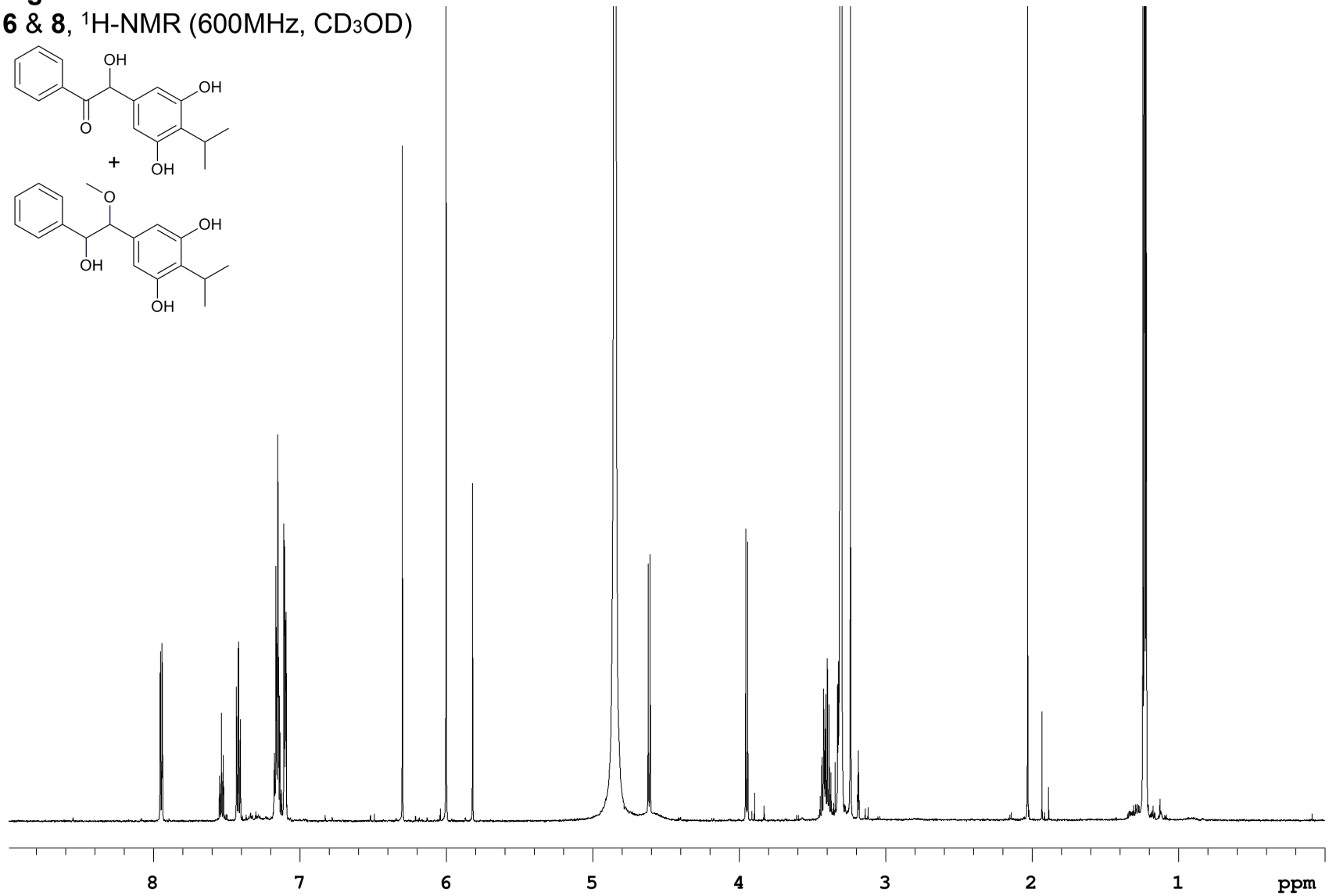

Figure S15
6 & **8**, gCOSY (600MHz, CD_3OD)

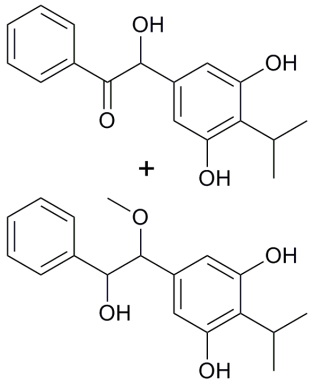

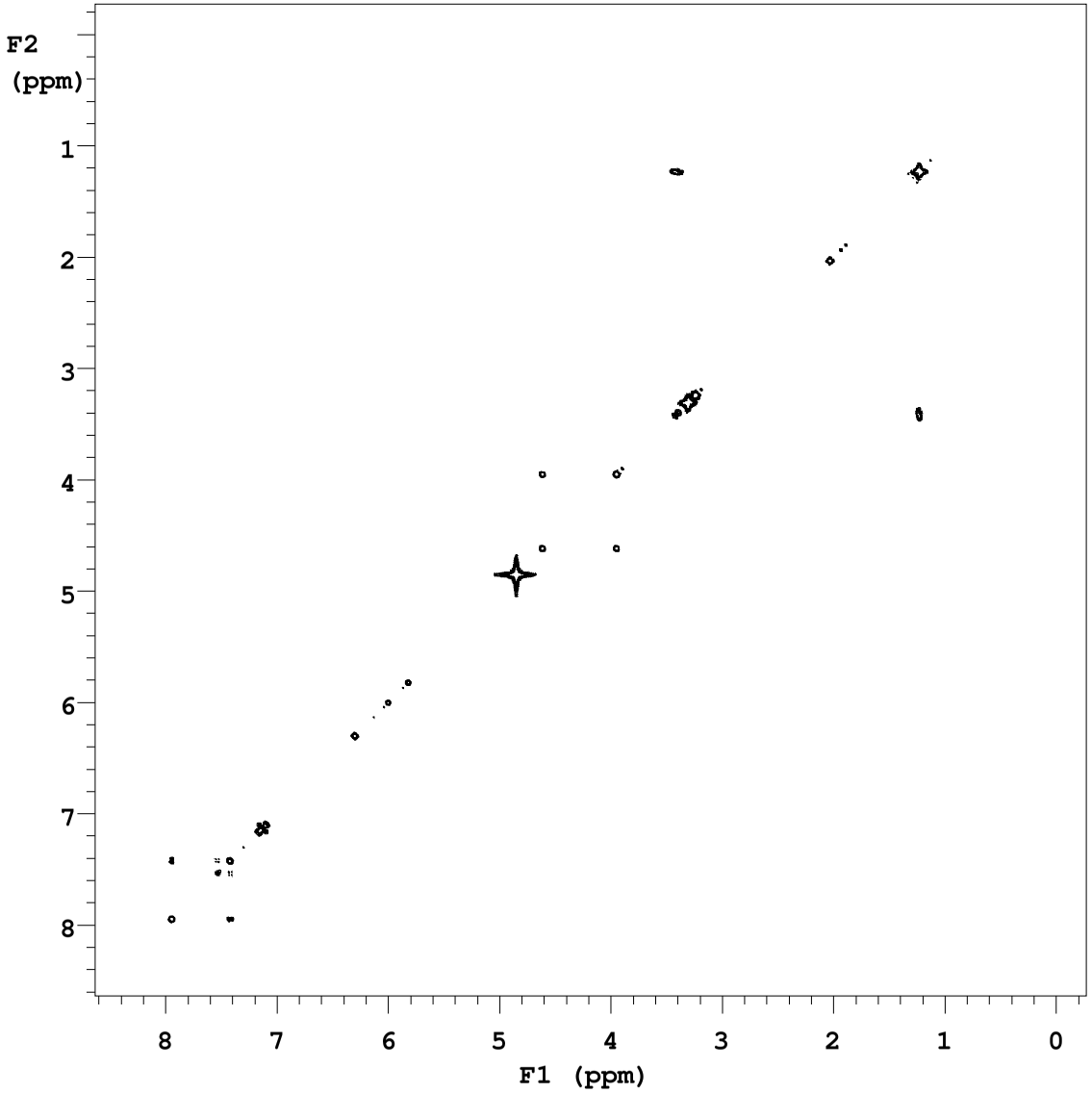

Figure S16

6 & **8**, gHSQC (600MHz, CD_3OD)

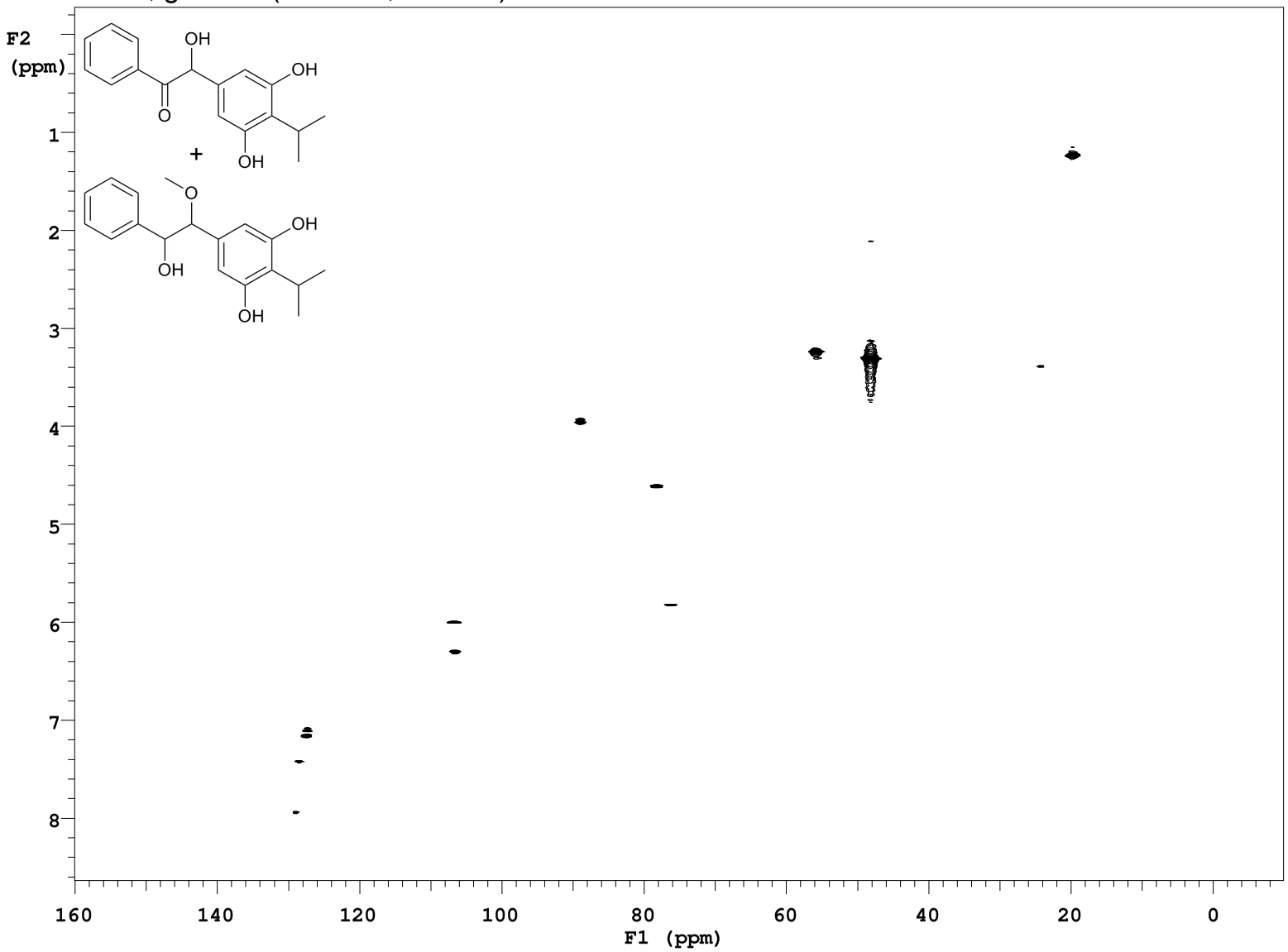

Figure S17
6 & **8**, gHMBC (600MHz, CD_3OD)

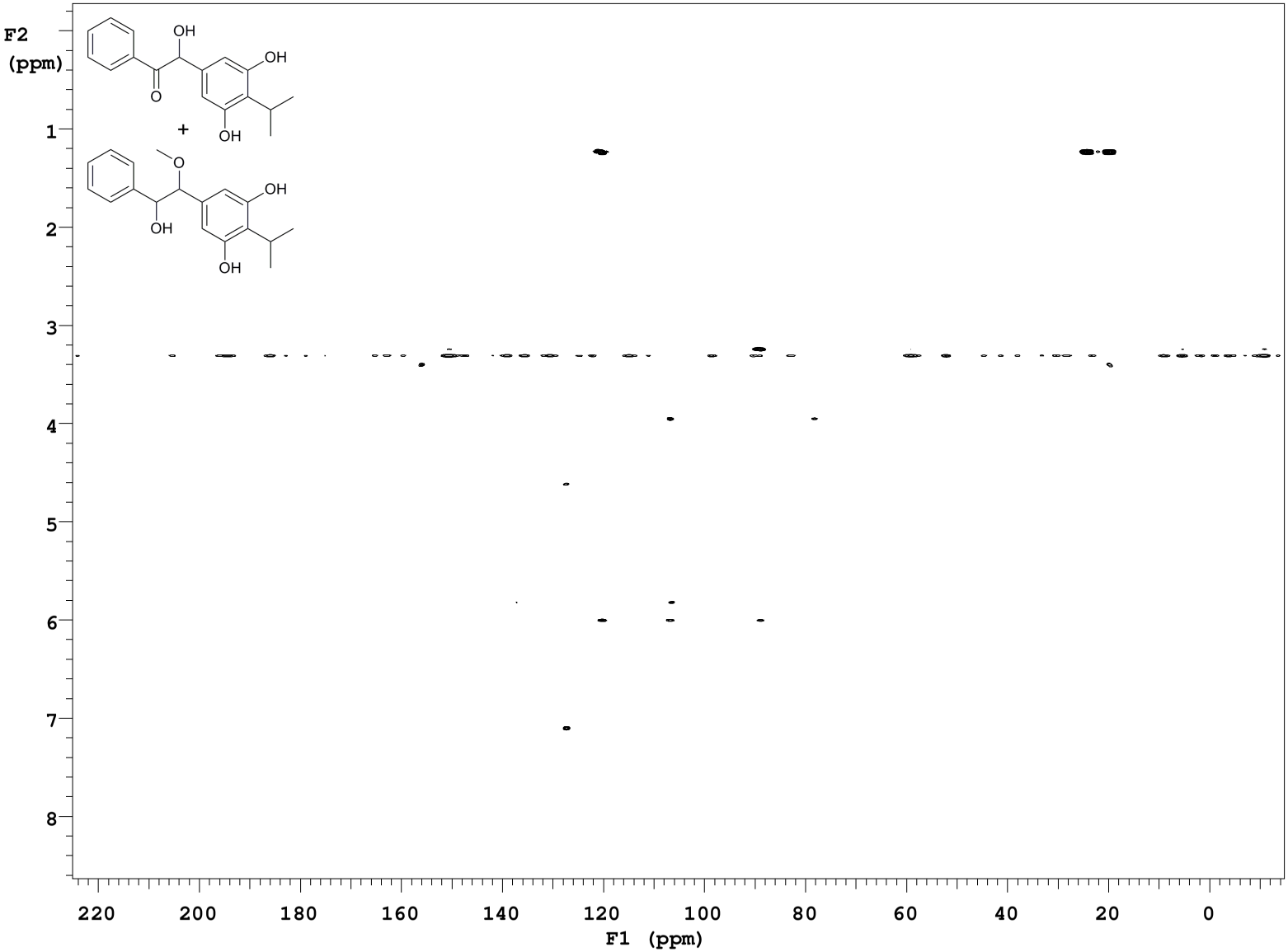

Figure S18

7, ^{1}H-NMR (600MHz, CD_3OD)

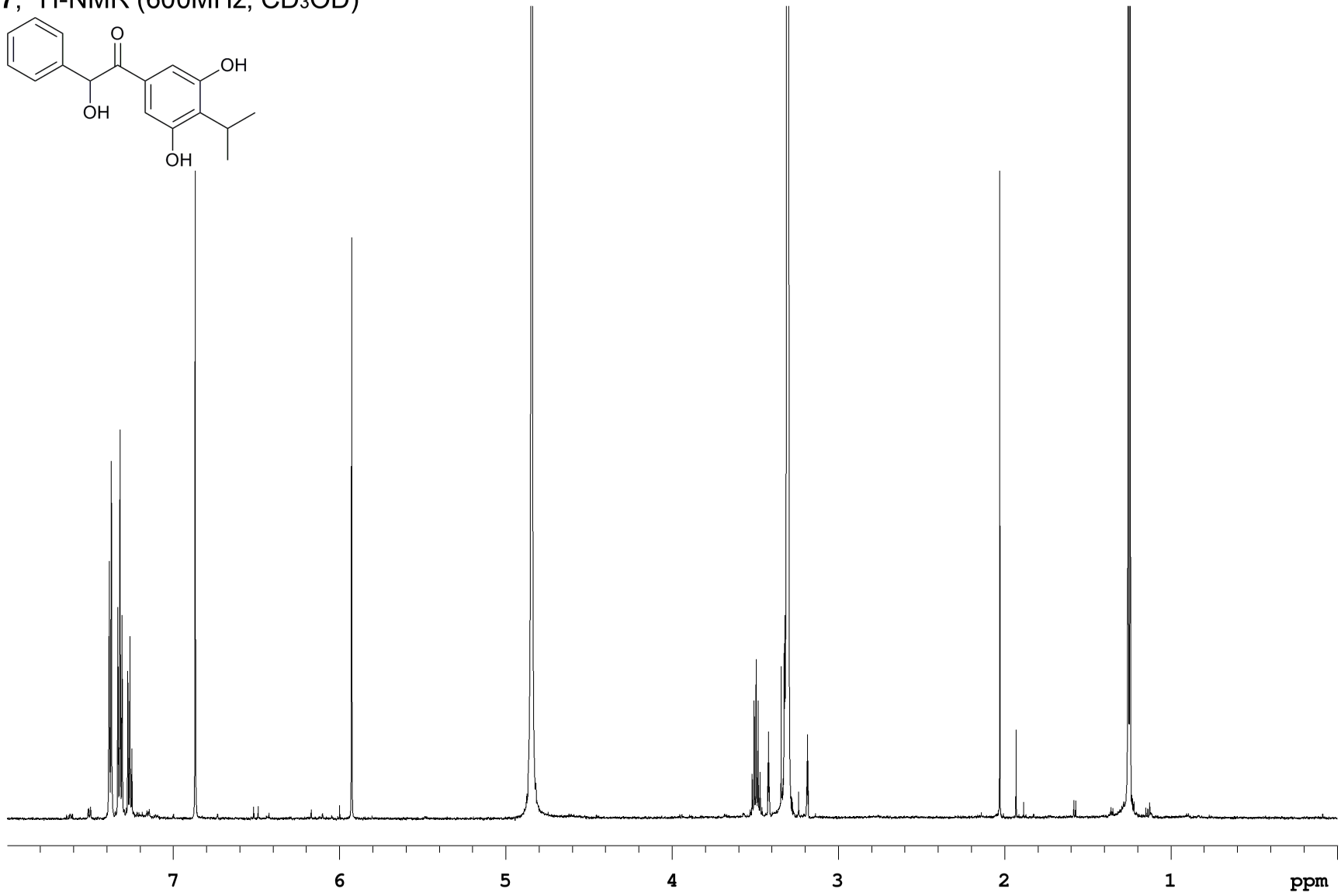

Figure S19

7, gCOSY (600MHz, CD_3OD)

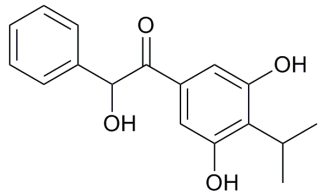

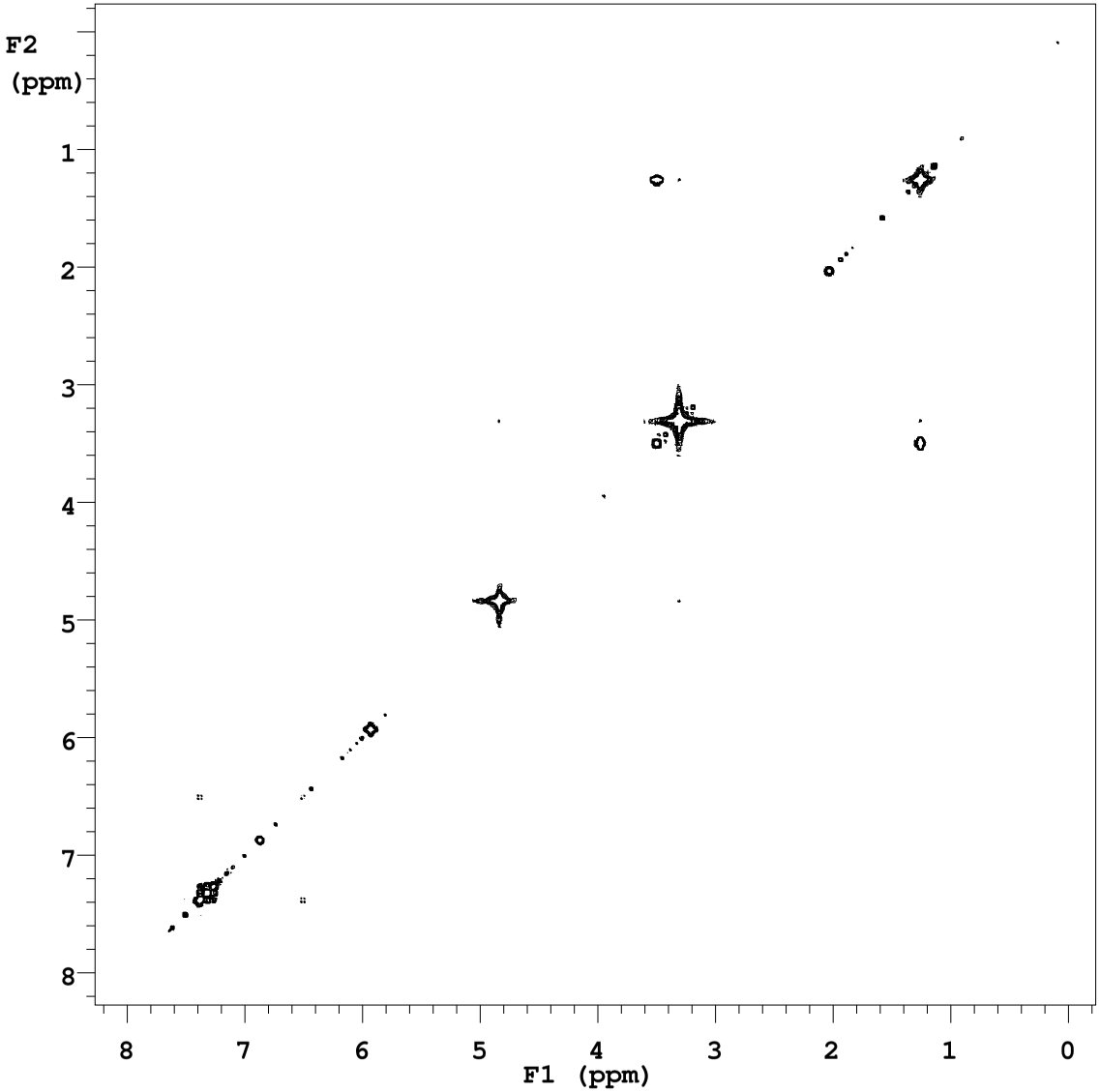

Figure S20

7, gHMBC (600MHz, CD_3OD)

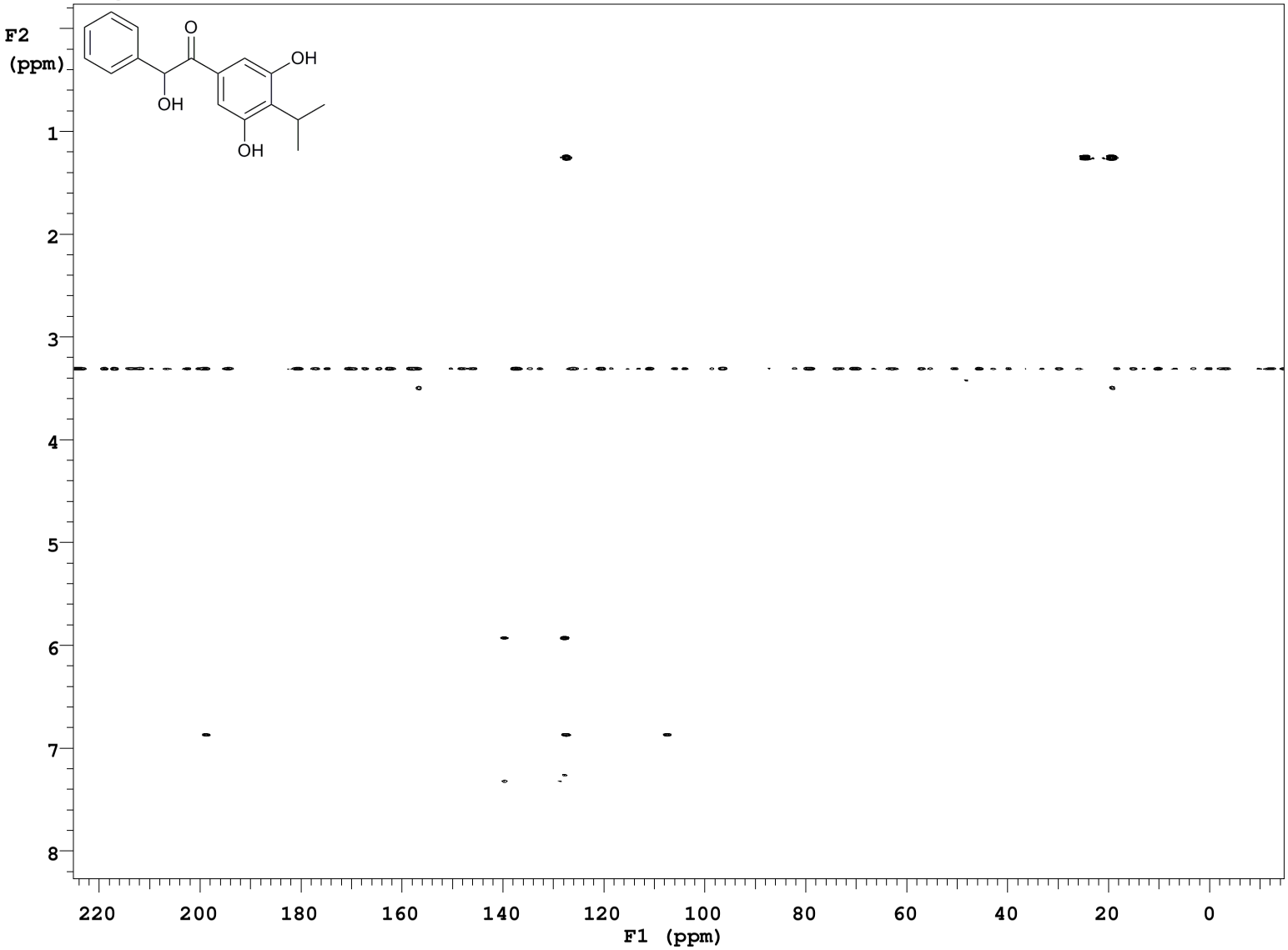

Figure S21

9, ^{1}H-NMR (600MHz, CD_3OD)

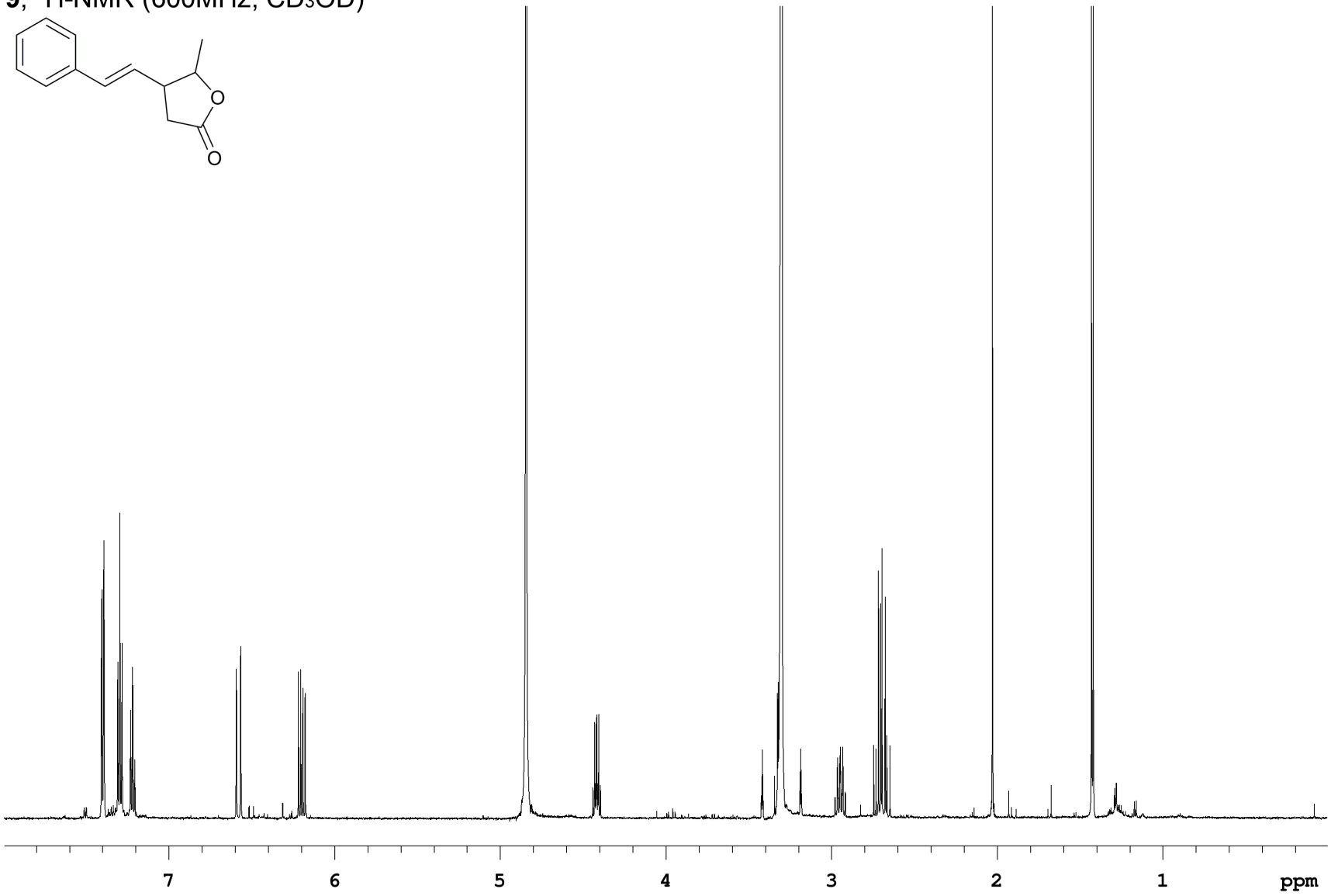

Figure S22
9, gCOSY (600MHz, CD_3OD)

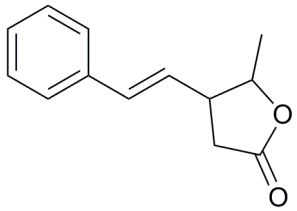

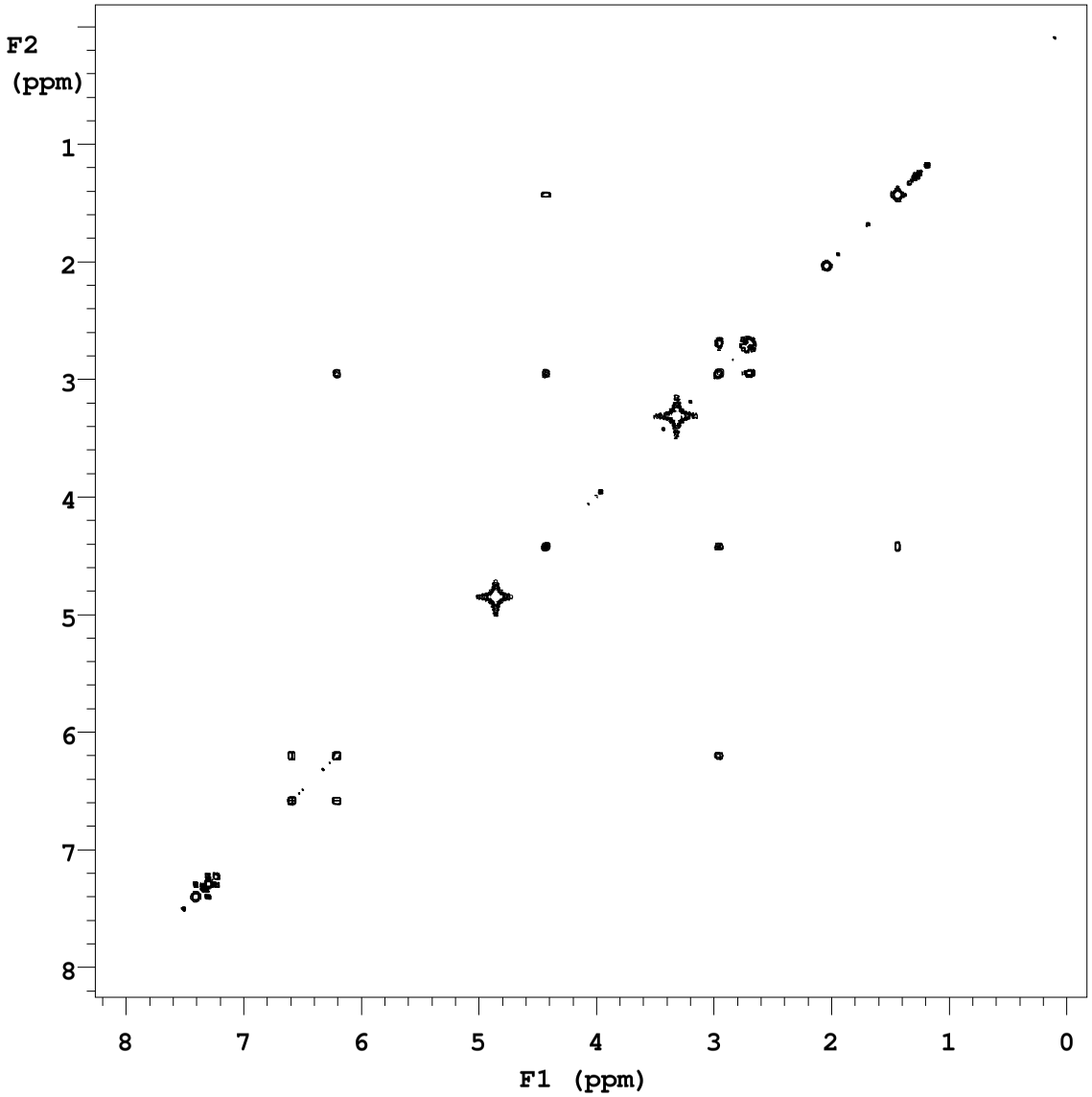

Figure S23

9, gHMQC (600MHz, CD_3OD)

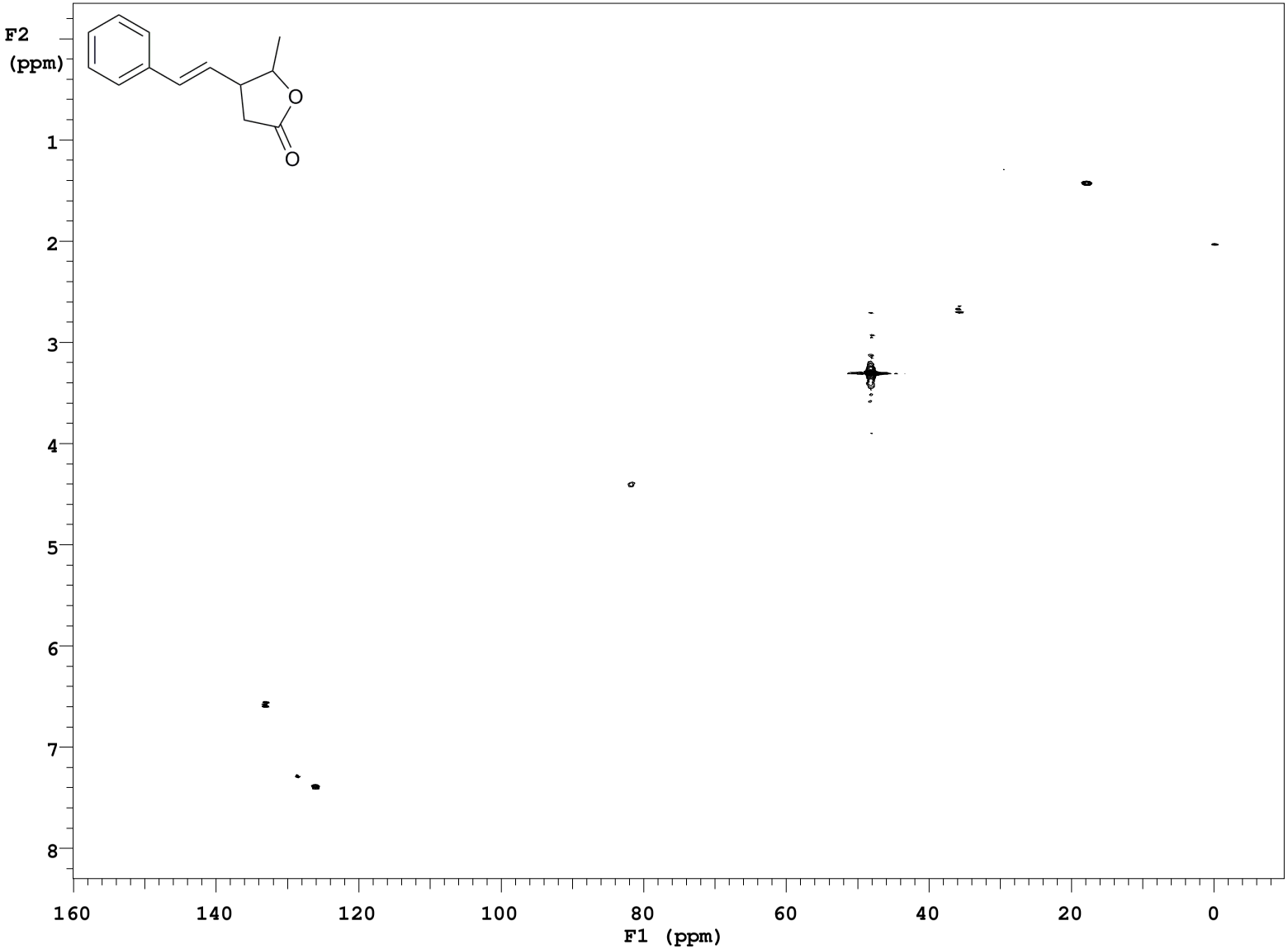

Figure S24

9, gHMBC (600MHz, CD_3OD)